ELSEVIER

BioSystems 63 (2001) 3–13

Bio Systems

www.elsevier.com/locate/biosystems

Bifurcation structure of a model of bursting pancreatic cells

Erik Mosekilde [a,*], Brian Lading [a], Sergiy Yanchuk [b], Yuri Maistrenko [b]

[a] *Department of Physics, Center for Chaos and Turbulence Studies, Building 309, The Technical University of Denmark, 2800 Kgs. Lyngby, Denmark*

[b] *Institute of Mathematics, National Academy of Sciences of Ukraine, Kiev 252601, Ukraine*

Abstract

One- and two-dimensional bifurcation studies of a prototypic model of bursting oscillations in pancreatic β-cells reveal a squid-formed area of chaotic dynamics in the parameter plane, with period-doubling bifurcations on one side of the arms and saddle-node bifurcations on the other. The transition from this structure to the so-called period-adding structure is found to involve a subcritical period-doubling bifurcation and the emergence of type-III intermittency. The period-adding transition itself is not smooth but consists of a saddle-node bifurcation in which $(n+1)$-spike bursting behavior is born, slightly overlapping with a subcritical period-doubling bifurcation in which n-spike bursting behavior loses its stability.

Keywords: Bursting cells; Period-adding; Bifurcations; Chaos; Basins of attraction

1. Introduction

By virtue of the far-from-equilibrium conditions in which they are maintained through the continuous action of ion pumps, many biological cells display an excitable electrical activity, or the membrane potential exhibits complicated patterns of slow and fast oscillations associated with variations in the ionic currents across the membrane. This dynamics plays an essential role for the function of the cell as well as for its communication with neighboring cells. It is well known, for instance, that pancreatic β-cells under normal circumstances display a bursting behavior with alternations between an active (spiking) state and a silent state (Dean and Matthews, 1970; Atwater and Beigelman, 1976; Meissner and Preissler, 1980). It is also established (Ozawa and Sand, 1986; Miura and Pernarowski, 1995) that the secretion of insulin depends on the fraction of time that the cells spend in the active state, and that this fraction increases with the concentration of glucose in the extracellular environment. The bursting dynamics controls the influx of Ca^{2+} ions into the cell, and calcium is considered an essential trigger for the release of insulin. In this way, the bursting dynamics organizes the response of the β-cells to varying glucose concentrations. At glucose concentrations below 5 mM, the cells do not burst at all. For high glucose concentrations (>22 mM), on the other hand, the cells spike continuously, and the secretion of insulin saturates (Satin and Cook, 1989).

* Corresponding author. Tel.: +45-45-253-104; Fax: +45-45-931-669.

E-mail address: ellen@chaos.fys.dtu.dk (E. Mosekilde).

0303-2647/01/$ - see front matter
PII: S0303-2647(01)00142-3

A number of experimental studies have shown that neighboring β-cells in an islet of Langerhans tend to synchronize their membrane activity (Sherman et al., 1988), and that cytoplasmic Ca^{2+} oscillations can propagate across clusters of β-cells in the presence of glucose (Gylfe et al., 1991). The precise mechanism underlying this interaction is not fully known. It is generally considered, however, that the exchange of ions via low impedance gap junctions between the cells play a significant role (Sherman and Rinzel, 1991). Such synchronization phenomena are important because not only do they influence the activity of the individual cell, but they also affect the overall insulin secretion. Actually, it appears that the isolated β-cell does not burst but shows disorganized spiking behavior as a result of the random opening and closing of potassium channels (Chay and Kang, 1988; Sherman et al., 1988; Smolen et al., 1993). A single β-cell may have of the order of a few hundred such channels. However, with typical opening probabilities as low as 5–10%, only a few tens will open during a particular spike. Organized bursting behavior arises for clusters of 20 or more closely coupled cells that share a sufficiently large number of ion channels for stochastic effects to be negligible.

Models of pancreatic β-cells are usually based on the standard Hodgkin–Huxley formalism with elaborations to account, for instance, for the intracellular storage of Ca^{2+}, for aspects of the glucose metabolism, or for the influence of ATP and other hormonal regulators. Over the years, many such models have been proposed with varying degrees of detail (Chay and Keizer, 1983; Chay, 1985a, 1990; Sherman and Rinzel, 1992). At the minimum, a three-dimensional model with two fast variables and one slow variable is required to generate a realistic bursting behavior. In the earliest models, the slow dynamics was often considered to be associated with changes in the intracellular Ca^{2+} concentration. It appears, however, that the correct biophysical interpretation of the slow variable remains unclear. The fast variables are usually the membrane potential V and the opening probability n of the potassium channels. More elaborate models with a couple of additional variables have also been proposed.

Although the different models have been around for quite some time, their bifurcation structure is so complicated as to not yet be understood in full. Conventional analyses (Sherman et al., 1988; Sherman, 1994) are usually based on a separation of the dynamics into a fast and a slow subsystem, whereafter the slow variable is treated as a bifurcation parameter for the fast dynamics. How compelling such an analysis may appear, particularly when one considers the large ratio of the involved time constants, the analysis fails to account for the more interesting dynamics of the models. Simulations with typical β-cell models display chaotic dynamics and period-doubling bifurcations for biologically interesting parameter values (Chay, 1985b; Fan and Chay, 1994), and such phenomena clearly cannot occur in a two-dimensional, time-continuous system such as the fast subsystem. The simplified analyses can also provide an incorrect account of the so-called period-adding transitions in which the system changes from a bursting behavior with n spikes per burst into a behavior with $n+1$ spikes per burst. Finally, the simplified analyses lead to a number of misperceptions with respect to the homoclinic bifurcations that control the onset of bursting.

Wang (1993) has proposed a combination of two different mechanisms to explain the emergence of chaotic bursting. First, the continuous spiking state undergoes a period-doubling cascade to a state of chaotic firing, and this state is destabilized in a boundary crisis. Bursting then arises through the realization of a homoclinic connection that serves as a reinjection mechanism for the chaotic saddle created in the boundary crisis. In this picture, the bursting oscillations are described as a form of intermittency with the silent state corresponding to the reinjection phase and the firing state to the normal laminar phase. Wang supports his analysis by a calculation of the escape rate from the chaotic saddle and he outlines a symbolic dynamics to characterize the various bursting states. As it appears, however, the question of how the homoclinic connection arises is left unanswered.

Terman (1991, 1992) has performed a more detailed analysis of the onset of bursting. He has

obtained a two-dimensional flow-defined map for the particularly complicated case where the equilibrium point of the full system falls close to a saddle point of the fast subsystem, which has a homoclinic orbit. By means of this map, Terman proved the existence of a hyperbolic structure (a chaotic saddle) similar in many ways to a Smale horseshoe. This represents an essential step forward in understanding the complexity involved in the emergence of bursting. However, since Terman's set is non-attracting, it cannot be related directly to the observed stable chaotic bursting phenomena.

More recently, Belykh et al. (2000) presented a qualitative analysis of a generic model structure that can reproduce the bursting and spiking dynamics of pancreatic β-cells. They consider four main scenarios for the onset of bursting. It is emphasized that each of these scenarios involves the formation of a homoclinic orbit that travels along the route of the bursting oscillations and, hence, cannot be explained in terms of bifurcations in the fast subsystem. In one of the scenarios, the bursting oscillations arise in a homoclinic bifurcation in which the one-dimensional stable manifold of a saddle point becomes attracting to its whole two-dimensional unstable manifold. This type of homoclinic bifurcation, and the complex behavior that it can produce, does not appear to have been examined previously.

Most recently, Lading et al. (2000) have studied chaotic synchronization (and the related phenomena of riddled basins of attraction, attractor bubbling, and on–off intermittency) for a model of two coupled, identical β-cells, and Yanchuk et al. (2000) have investigated the effects of a small parameter mismatch between the coupled chaotic oscillators. In the limit of strong interaction, it was found that such a mismatch gives rise to a shift of the synchronized state away from the symmetric synchronization manifold, combined with occasional bursts out of synchrony. This whole class of phenomena is of significant interest to the biological sciences (Kaneko, 1994) where one often encounters the situation that a large number of cells (or functional units), which each performs complicated non-linear oscillations, interact to produce a coordinated function on a higher organizational level.

The purpose of the present paper is to give a somewhat simpler account of the bifurcation structure of the individual β-cell. Our analysis reveals the existence of a squid-formed area of chaotic dynamics in parameter plane with period-doubling cascades along one side of the arms and saddle-node bifurcations along the other. The transition from this structure to the so-called period-adding structure involves a subcritical period-doubling bifurcation and the emergence of type-III intermittency. The period-adding transition itself is found to be non-smooth and to consist of a saddle-node bifurcation in which stable $(n+1)$-spike behavior is born, overlapping slightly with a subcritical period-doubling bifurcation in which stable n-spike behavior ceases to exist. The two types of behavior follow each other closely in phase space over a major part of the orbit to suddenly depart and allow one of the solutions to perform an extra spike.

Bursting behavior similar to the dynamics that we have described for pancreatic β-cells is known to occur in a variety of other cell types as well. Pant and Kim (1976), for instance, have developed a mathematical model to account for experimentally observed burst patterns in pacemaker neurons, and Morris and Lecar (1981) have modelled the complex firing patterns in barnacle giant muscle fibers. Braun et al. (1980) have investigated bursting patterns in discharging cold fibers of the cat, and Braun et al. (1994) have studied the effect of noise on signal transduction in shark sensory cells. Although the biophysical mechanism underlying the bursting behavior may vary significantly from cell type to cell type, we expect many of the basic bifurcation phenomena to remain the same.

2. The bursting cell model

As the basis for the present analysis, we shall use the following model suggested by Sherman et al. (1988):

$$\tau\frac{\mathrm{d}V}{\mathrm{d}t} = -I_{\mathrm{Ca}}(V) - I_{\mathrm{K}}(V,n) - g_S S(V - V_{\mathrm{K}}) \qquad (1)$$

with

$$\tau\frac{dn}{dt} = \sigma[n_\infty(V) - n] \tag{2}$$

$$\tau_S\frac{dS}{dt} = S_\infty(V) - S \tag{3}$$

$$I_{Ca}(V) = g_{Ca}m_\infty(V)(V - V_{Ca}) \tag{4}$$

$$I_K(V,n) = g_K n(V - V_K) \tag{5}$$

$$w_\infty(V) = \left[1 + \exp\left\{\frac{V_w - V}{\theta_w}\right\}\right]^{-1}$$

$$\text{for } w = m,\ n \text{ and } S \tag{6}$$

Here, V represents the membrane potential, n may be interpreted as the opening probability of the potassium channels, and S accounts for the presence of a slow dynamics in the system. As previously noted, the correct biophysical interpretation of this variable remains uncertain. I_{Ca} and I_K are the calcium and potassium currents, $g_{Ca} = 3.6$ and $g_K = 10.0$ are the associated conductances, and $V_{Ca} = 25$ and $V_K = -75$ mV are the respective Nernst (or reversal) potentials. τ/τ_S defines the ratio of the fast (V and n) and the slow (S) time scales. The time constant for the membrane potential is determined by the capacitance and the typical total conductance of the cell membrane. With $\tau = 0.02$ s and $\tau_S = 35$ s, the ratio $k_S = \tau/\tau_S$ is quite small, and the cell model is numerically stiff.

The calcium current I_{Ca} is assumed to adjust instantaneously to variations in V. For fixed values of the membrane potential, the gating variables n and S relax exponentially towards the voltage-dependent steady-state values $n_\infty(V)$ and $S_\infty(V)$. Together with the ratio k_S of the fast to the slow time constant, V_S will be used as the main bifurcation parameter. This parameter determines the membrane potential at which the steady-state value for the gating variable S attains one-half of its maximum value. The other parameters are $g_S = 4.0$, $V_m = -20$ mV, $V_n = -16$ mV, $\theta_m = 12$ mV, $\theta_n = 5.6$ mV, $\theta_S = 10$ mV, and $\sigma = 0.85$. These values are all adjusted to fit experimentally observed relationships. In accordance with the formulation used by Sherman et al. (1988), there is no capacitance in Eq. (1), and all the conductances are dimensionless. To eliminate a dependence on the cell size, all conductances have been scaled with the typical conductance. Hence, we may consider the model as a model of a cluster of closely coupled β-cells that share the combined capacity and conductance of the entire membrane area.

Fig. 1 shows an example of the temporal variations of the variables V, n and S as obtained by simulating the cell model under conditions where it exhibits continuous chaotic spiking. Here, $k_S = 0.57 \times 10^{-3}$ and $V_S = -38.34$ mV. We notice the extremely rapid opening and closing of some of the potassium channels. The opening probability n changes from nearly nothing to about 10% at the peak of each spike. We also notice how the slow variable increases during the bursting phase to reach a value just below 310, whereafter the cell switches into the silent phase, and S gradually relaxes back. If the slow variable is assumed to represent the intracellular Ca^{2+} concentration, this concentration is seen to increase during each spike until it reaches a threshold, and the bursting phase is switched off. S hereafter decreases as Ca^{2+} is continuously pumped out of the cell.

Let us start our bifurcation analysis with a few comments concerning the equilibrium points of the β-cell model. The zero points of the vector field Eqs. (1)–(3) are given by:

$$g_{Ca}m_\infty(V)(V - V_{Ca}) + g_K n(V - V_K) + g_S S(V - V_K) = 0 \tag{7}$$

$$n = n_\infty(V) = \left[1 + \exp\left(\frac{V_n - V}{\theta_n}\right)\right]^{-1} \tag{8}$$

$$S = S_\infty(V) = \left[1 + \exp\left(\frac{V_S - V}{\theta_S}\right)\right]^{-1} \tag{9}$$

so that the equilibrium values of n and S are uniquely determined by V. Substituting Eqs. (8) and (9) into Eq. (7), the equation for the equilibrium potential becomes

$$f(V) \equiv g_{Ca}m_\infty(V)(V - V_{Ca}) + g_K n_\infty(V)(V - V_K) + g_S S_\infty(V)(V - V_K) = 0 \tag{10}$$

with $m_\infty(V)$ as given by Eq. (6). Assuming $V_{Ca} > V_K$ and considering the conductances g_{Ca}, g_K and g_S to be positive by definition, we observe that any equilibrium point of the β-cell model must have a membrane potential in the interval $V_K <$

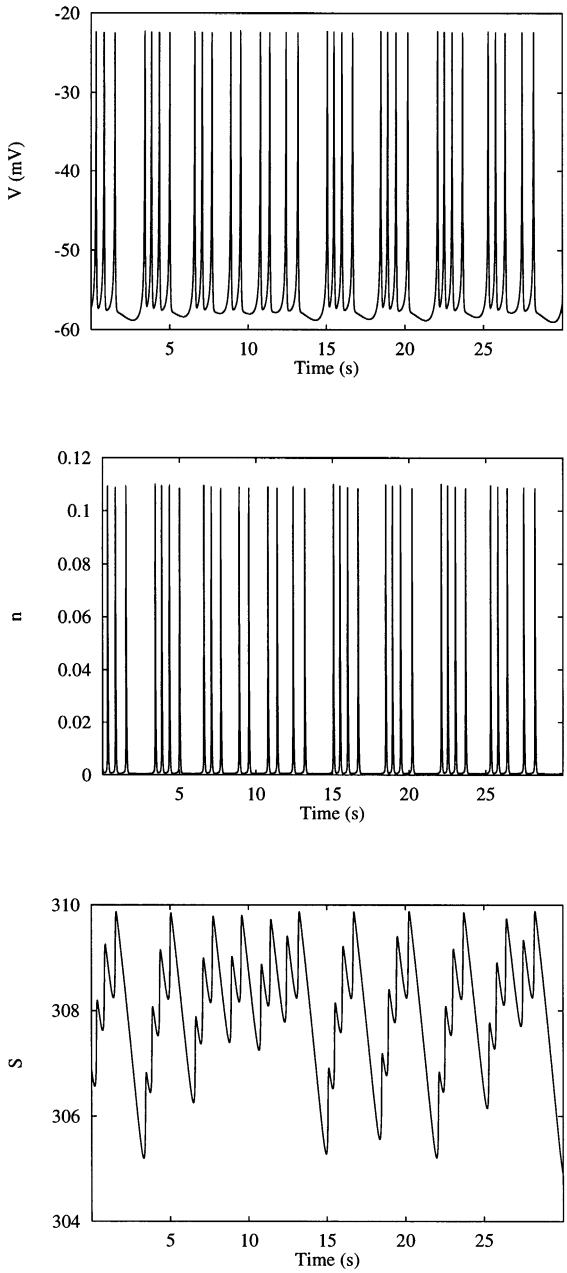

Fig. 1. Example of the temporal variations of the membrane potential $V(t)$, the opening probability $n(t)$ for the potassium channels, and the slow variable $S(t)$ that controls the switching between the active and the silent phases. $k_S = 0.57 \times 10^{-3}$ and $V_S = -38.34$ mV. The model exhibits continuous chaotic spiking. Here and in all of the following figures, $S(t)$ has been multiplied by a factor of τ_S/τ.

$V < V_{Ca}$, and that there must be at least one such point. This assertion follows directly from the continuity of $f(V)$ as defined from Eq. (10). For $V < V_K$, all terms in the expression for $f(V)$ are negative, and $f(V) < 0$. For $V > V_{Ca}$, all terms in $f(V)$ are positive. Hence, there is at least one root of Eq. (10) in the interval between V_K and V_{Ca}, and no roots outside this interval.

Evaluated at such an equilibrium point, the Jacobian matrix for the β-cell model has the form:

$$J = \begin{Bmatrix} J_{11} & J_{12} & J_{13} \\ J_{21} & J_{22} & 0 \\ J_{31} & 0 & J_{33} \end{Bmatrix} \tag{11}$$

with

$$J_{11} = -g_{Ca}\frac{\partial m_\infty(V)}{\partial V}(V - V_{Ca}) - g_{Ca} m_\infty(V)\frac{V_{Ca} - V_K}{V - V_K} \tag{12}$$

$$J_{12} = -g_K(V - V_K) \tag{13}$$

$$J_{13} = -g_S k_S(V - V_K) \tag{14}$$

$$J_{21} = \sigma\frac{\partial n_\infty(V)}{\partial V} \tag{15}$$

$$J_{22} = -\sigma \tag{16}$$

$$J_{31} = \frac{\partial S_\infty(V)}{\partial V} \tag{17}$$

and

$$J_{33} = -k_S \tag{18}$$

Applying Hurwitz' theorem (which gives the conditions for all solutions of the characteristic equation to have negative real parts), we obtain the following criteria for the equilibrium point to be asymptotically stable:

$$J_{11} + J_{22} + J_{33} < 0 \tag{19}$$

and

$$(J_{11} + J_{22} + J_{33})(J_{11}\ J_{33} + J_{11}\ J_{22} + J_{22}\ J_{33}) + J_{31}\ J_{22}\ J_{13} + J_{21}\ J_{12}\ J_{33} < 0 \tag{20}$$

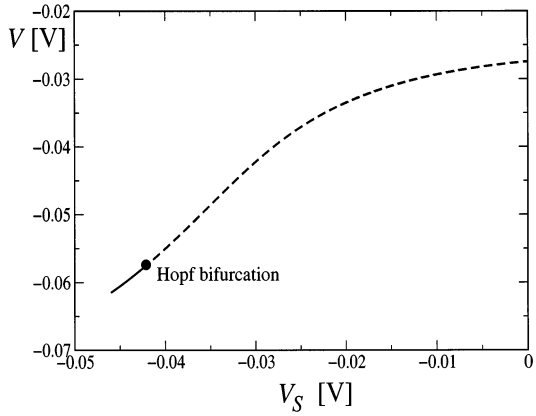

Fig. 2. Bifurcation diagram for the bursting cell model as obtained by means of one-dimensional continuation methods. The equilibrium point undergoes a Hopf bifurcation for $V_S \cong -42$ mV. $k_S = 0.1$.

For a characteristic equation of third-order $a_0x^3 + a_1x^2 + a_2x + a_3 = 0$ with $a_0 > 0$, we have the Hurwitz' conditions

$$a_1 > 0, \qquad \begin{vmatrix} a_1 & a_0 \\ a_3 & a_2 \end{vmatrix} > 0, \qquad \text{and} \qquad a_3 > 0 \tag{21}$$

To derive the conditions of Eqs. (19) and (20), we only have to substitute the coefficients of our characteristic equation into Eq. (21), noting that the condition $a_3 > 0$ will always be satisfied with the assumed parameter values.

For a Hopf bifurcation to occur, the second condition in Eq. (21) must be violated. As shown in the bifurcation diagram of Fig. 2, this may happen as V_S is increased. Here, we have plotted the equilibrium membrane potential as a function of V_S for $k_S = 0.1$. All other parameters assume their standard values. For low values of V_S (fully-drawn curve in the bifurcation diagram), the equilibrium point is asymptotically stable. At $V_S \cong -42$ mV, however, the model undergoes a Hopf bifurcation, and the equilibrium point turns into an unstable focus. The stable as well as the unstable branch of the bifurcation curve was followed by means of standard continuation methods. Due to the stiffness of the model, such methods are not always easy to apply. In the next section, we shall investigate the main structure of the subsequent bifurcations.

3. Bifurcation diagrams for the cell model

Fig. 3 shows a one-dimensional bifurcation diagram for the cell model with V_S as the control parameter. Here, $k_S = 0.57 \times 10^{-3}$. The figure resembles figures that one can find in early papers by Chay (1985b). The diagram was constructed from a Poincaré section in phase space with $n = 0.04$. With this section, we can ensure that all spikes performed by the model are recorded. For $V_S > -37.8$ mV, the model exhibits continuous periodic spiking. As V_S is reduced, the spiking state undergoes a usual period-doubling cascade to chaos with periodic windows. Each window is terminated by a saddle-node bifurcation to the right and by a period-doubling cascade to the left.

Around $V_S = -38.3$ mV, a dramatic change in the size of the chaotic attractor takes place. This marks the transition to bursting dynamics through the formation of a homoclinic connection in three-dimensional phase space (Belykh et al., 2000). Below $V_S \cong -38.5$ mV the bifurcation scenario is reversed, and for $V_S \cong -38.9$ mV a backwards period-doubling cascade leads the system into a state of periodic bursting with five spikes per burst. The interval of periodic bursting ends near $V_S = -39.7$ mV in a saddle-node leading to chaos in the form of type-I intermittency (Bergé et al., 1984). With further reduction of V_S, the chaotic dynamics develops via a new

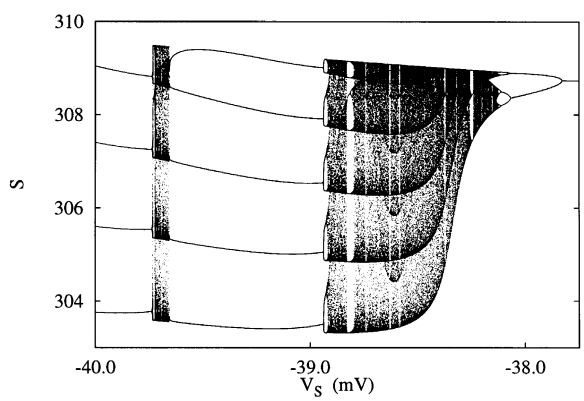

Fig. 3. One-dimensional bifurcation diagram for $k_S = 0.57 \times 10^{-3}$. The model displays chaotic dynamics in the transition intervals between continuous periodic spiking and bursting, and between the main states of periodic bursting.

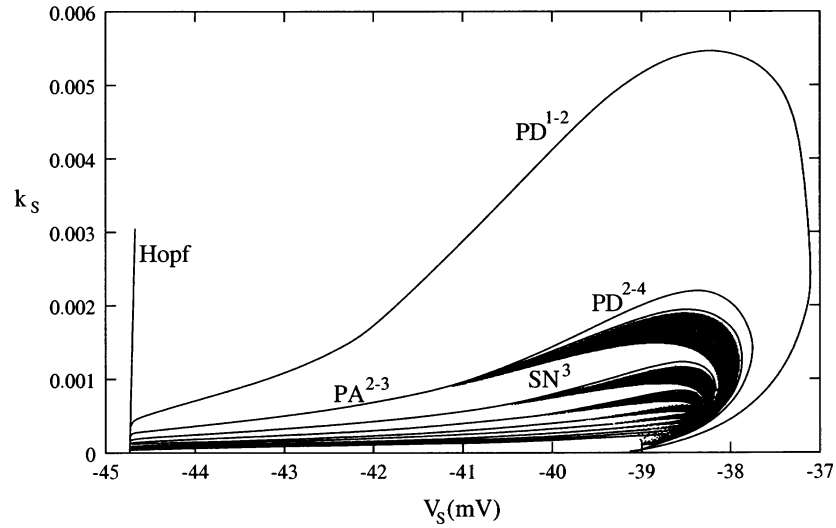

Fig. 4. Two-dimensional bifurcation diagram outlining the main bifurcation structure in the (V_S, k_S) parameter plane. Note the squid-formed black region with chaotic dynamics.

reverse period-doubling cascade into periodic bursting with four spikes per burst. It is clear from this description that chaotic dynamics tends to arise in the transitions between continuous spiking and bursting, and between the different bursting states.

To establish a more complete picture of the bifurcation structure, we have applied a large number of such one-dimensional scans to identify the main periodic solutions (up to period 10) and to locate and classify the associated bifurcations. The results of this investigation are displayed in the two-dimensional bifurcation diagram of Fig. 4. To the left in this figure, we observe the Hopf bifurcation curve discussed in Section 2. Below this curve, the model has one or more stable equilibrium points. Above the curve, we find a region of complex behavior delineated by the period-doubling curve PD^{1-2}. Along this curve, the first period-doubling of the continuous spiking behavior takes place. In the heart of the region surrounded by PD^{1-2} we find an interesting squid-formed structure with arms of chaotic behavior (indicated black) stretching down towards the Hopf bifurcation curve.

Each of the arms of the squid-formed structure separates a region of periodic bursting behavior with n spikes per burst from a region with regular $(n+1)$-spikes per burst behavior. Each arm has a period-doubling cascade leading to chaos on one side and a saddle-node bifurcation on the other. It is easy to see that the number of spikes per burst must become very large as k_S approaches zero. Fig. 5 is a magnification of part of the two-dimensional bifurcation diagram. Here, we observe how the chaotic region in the arms narrows down as the bifurcation curves on both sides approach one another with decreasing values of V_S. This leads to the so-called period-adding structure (Chay, 1985b). Along the curves of this structure, a periodic bursting state with n spikes per burst appears to be directly transformed into a state with $n+1$ spikes per burst.

To illustrates what happens in this transition, Figs. 6 and 7 show one-dimensional bifurcation diagrams obtained by scanning from the two spikes per burst regime into the three spikes per burst regime for $k_S = 1.0 \times 10^{-3}$ and $k_S = 0.84 \times 10^{-3}$, respectively. To the left in Fig. 6, we find two spikes per burst behavior, and to the right we have periodic bursting with three spikes per burst. As V_S is gradually increased from -40.86 mV, the two spikes per burst behavior remains stable all the way up to $V_S \cong -40.827$ mV, where it

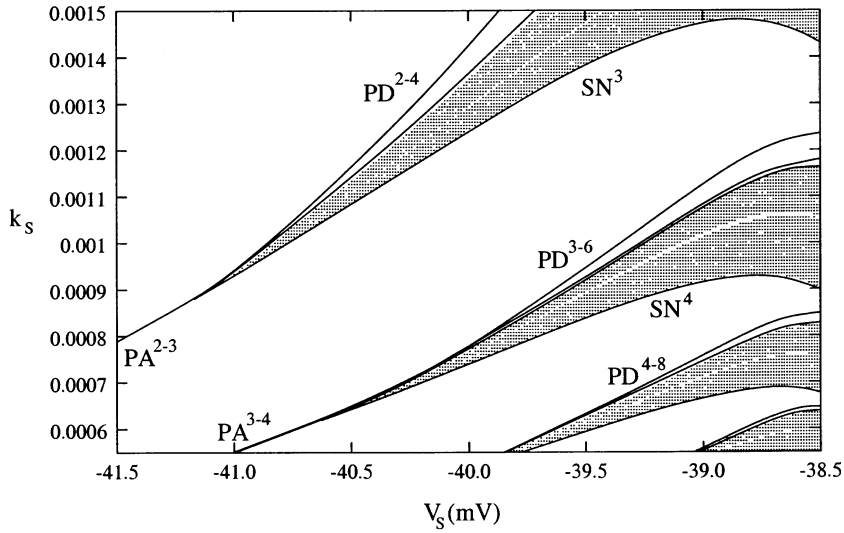

Fig. 5. Magnification of part of the bifurcation diagram in Fig. 4. Note how the chaotic region in each squid arm narrows down as the bifurcation curves on both sides approach one another and intersect.

undergoes a subcritical period-doubling. In the absence of another attracting state in the neighborhood, the system explodes into a state of Type-III intermittency (Bergé et al., 1984). The reinjection mechanism associated with this intermittency behavior may correspond to the reinjection mechanism proposed by Wang (1993).

If we go backwards in the bifurcation diagram of Fig. 6, the unstable period-4 solution generated in the subcritical period-doubling bifurcation stabilizes in a saddle-node bifurcation near $V_S = -40.851$ mV, and with increasing values of V_S the stable period-4 solution undergoes a period-doubling cascade to chaos. Around $V_S = -40.841$ mV, the chaotic attractor disappears in a boundary crisis as it collides with the inset to the unstable period-4 solution. This process is likely to leave a chaotic saddle that can influence the dynamics in the intermittency regime for $V_S > -40.827$ mV. For higher values of V_S, the chaotic state (with periodic windows) continues to exist until the saddle-node bifurcation at $V_S \cong -40.765$ mV where periodic bursting with three spikes per burst emerges.

Fig. 7 shows a brute-force bifurcation diagram obtained by scanning V_S in both directions across the PA$^{2-3}$ period-adding "curve" for $k_S = 0.84 \times 10^{-3}$. Inspection of this figure clearly reveals the narrow interval around $V_S = -41.43$ mV where the two-spike and three-spike solutions coexist. Evaluation of the eigenvalues shows that the two-spike solution disappears in a (subcritical) period-doubling bifurcation and that the stable three-spike solution arises in a saddle-node bifurcation. In the next period-adding transition (PA$^{3-4}$),

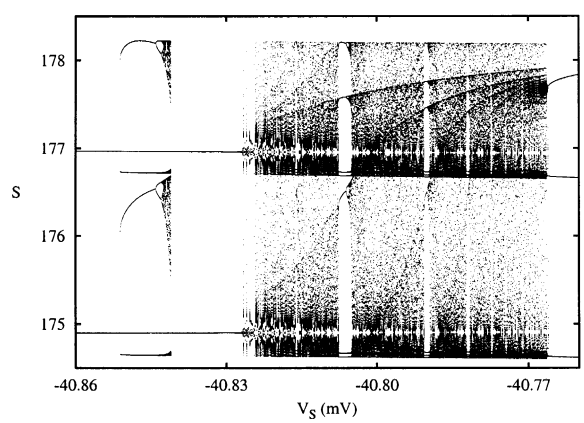

Fig. 6. One-dimensional bifurcation diagram obtained by scanning from the two spikes per burst regime into the three spikes per burst regime for $k_S = 1.0 \times 10^{-3}$. Note the subcritical period-doubling and the associated transition to type-III intermittency for $V_S \cong -40.827$ mV.

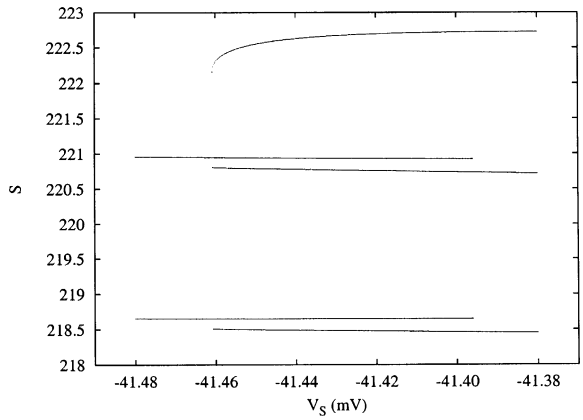

Fig. 7. One-dimensional bifurcation diagram obtained by scanning V_S in both directions across the PA^{2-3} period-adding curve in Fig. 4. $k_S = 0.84 \times 10^{-3}$. Note the interval of coexisting two-spike and three-spike solutions.

the three-spike solution undergoes a subcritical period-doubling, and a four-spike solution emerges in a saddle-node bifurcation. Again, there is a small interval of coexistence between the two solutions. This is a very different scenario from the continuous transition from n-spike behavior to $(n+1)$-spike behavior described by Terman (1991, 1992).

Fig. 8 shows a phase space projection of the coexisting two-spike and three-spikes solutions that one can observe for $V_S = -42.0$ mV and $k_S = 0.669 \times 10^{-3}$. Note how these solutions follow one another very closely for part of the cycle to sharply depart at a point near $V = -57$ mV and $S = 264$. Hence, with a slightly smaller numerical accuracy, it may appear as if the two solutions smoothly transform into one another. Fig. 9 displays the basins of attraction for the two coexisting solutions. Here, initial conditions attracted to the two-spike solution are marked black, and initial conditions from which the trajectory approaches the three-spike solution are left blank. The figure was constructed for initial values of the fast gate variable of $n = 0.04$. Finally, Fig. 10 shows a magnification of part of the basin boundary in Fig. 9 around $V = -50$ mV and $S = 210.2$. Inspection of this magnification clearly reveals the fractal structure of the basin boundary with the characteristic set of bands of rapidly decreasing width.

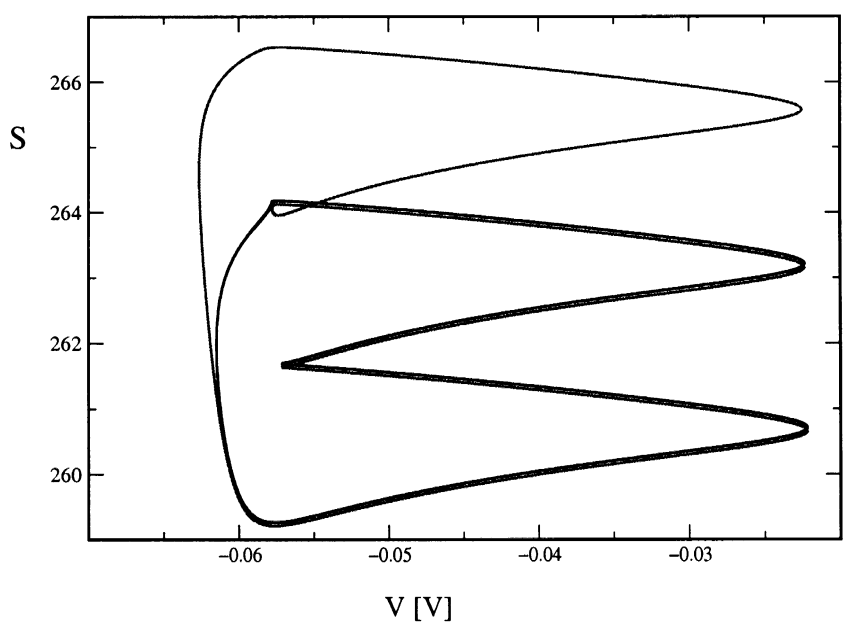

Fig. 8. Phase space projection of the coexisting two-spike and three-spike solutions for $V_S = -42.0$ mV and $k_S = 0.669 \times 10^{-3}$. Note the sharp point of departure between the two solutions.

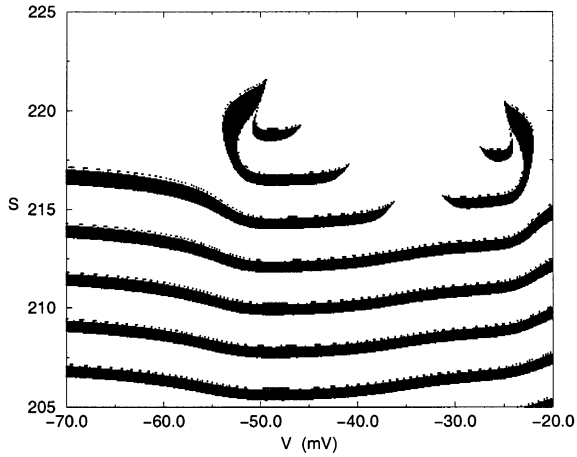

Fig. 9. Basins of attraction for the coexisting two-spike and three-spike solutions for $k_S = 0.84 \times 10^{-3}$. Initial conditions from which the trajectory approaches the two spikes per burst solution are marked black.

4. Conclusion

We have presented a bifurcation analysis of a three-variable model that can produce the characteristic bursting and spiking behavior of pancreatic β-cells. A more mathematically oriented description of the homoclinic bifurcations leading to bursting has been given elsewhere (Belykh et al., 2000). Our main observations were:

1. a squid-formed regime of chaotic dynamics may exist in parameter plane inside the region surrounded by the first period-doubling curve for the periodic spiking behavior. The arms of this squid separate regions of different number of spikes per burst;
2. each arm has a structure with a period-doubling cascade on one side and a saddle-node bifurcation on the other;
3. towards the end of the arm, the first period-doubling bifurcation tends to become subcritical: in a certain parameter region, this gives rise to a chaotic boundary crisis followed by a transition to type-III intermittency; and
4. the so-called period-adding structure arises when the subcritical period-doubling curve intersects the saddle-node bifurcation curve on the other side of the arm. This leads to a region of coexistence of stable n-spikes and $(n+1)$-spike behavior.

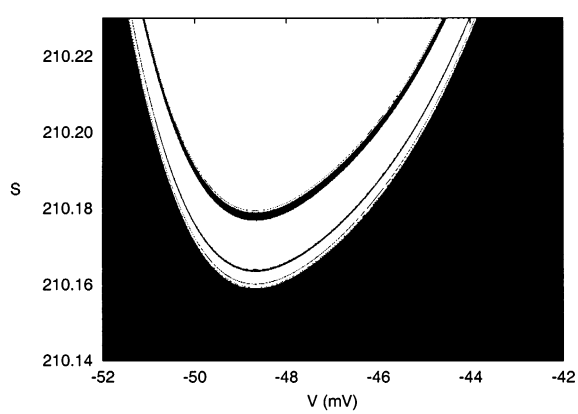

Fig. 10. Magnification of part of the basin boundary in Fig. 9 illustrating the characteristic fractal nature of this boundary.

These results appear to be at odds with the results usually found in the literature (Terman, 1991). It is obvious that different results may be obtained with different models and different parameter settings. However, the consistency in our bifurcation scenarios seems to imply that similar scenarios may also be found in other bursting cell models.

References

Atwater, I., Beigelman, P.M., 1976. Dynamic characteristics of electrical activity in pancreatic β-cells. J. Physiol. (Paris) 72, 769–786.

Belykh, V.N., Belykh, I.V., Colding-Jøgensen, M., Mosekilde, E., 2000. Homoclinic bifurcations leading to the emergence of bursting oscillations in cell models. Eur. J. Phys. E 3, 205–219.

Bergé, P., Pomeau, Y., Vidal, C., 1984. Order Within Chaos: Towards a Deterministic Approach to Thrbulence. Wiley, New York.

Braun, H.A., Bade, H., Hensel, H., 1980. Static and dynamic discharge patterns of bursting cold fibers related to hypothetical receptor mechanisms. Pflügers Arch. 386, 1–9.

Braun, H.A., Wissing, H., Schäfer, K., Hirsch, M.C., 1994. Oscillation and noise determine signal transduction in shark multimodal sensory cells. Nature 367, 270–273.

Chay, T.R., Kang, H.S., 1988. Role of single-channel stochastic noise on burstmg clusters of pancreatic β-cells. Biophys. J. 54, 427–435.

Chay, T.R., Keizer, J., 1983. Minimal model for membrane oscillations in the pancreatic β-cell. Biophys. J. 42, 181–190.

Chay, T.R., 1985a. Glucose response to bursting-spiking pancreatic β-cells by a barrier kinetic model. Biol. Cybern. 52, 339–349.

Chay, T.R., 1985b. Chaos in a three-variable model of an excitable cell. Physica D 16, 233–242.

Chay, T.R., 1990. Bursting excitable cell models by a slow Ca^{2+} current. J. Theor. Biol. 142, 305–315.

Dean, P.M., Matthews, E.K., 1970. Glucose induced electrical activity in pancreatic islet cells. J. Physiol. (Lond.) 210, 255–264.

Fan, Y.-S., Chay, T.R., 1994. Generation of periodic and chaotic bursting in an excitable cell model. Biol. Cybern. 71, 417–431.

Gylfe, E., Grapengiesser, E., Hellman, B., 1991. Propagation of cytoplasmic Ca^{2+} oscillations in clusters of pancreatic β-cells exposed to glucose. Cell Calcium 12, 229–240.

Kaneko, K., 1994. Relevance of dynamic clustering to biological networks. Physica D 75, 55–73.

Lading, B., Mosekilde, E., Yanchuk, S., Maistrenko, Y., 2000. Chaotic synchronization between coupled pancreatic β-cells. Prog. Theor. Phys. Suppl. 139, 164–177.

Meissner, H.P., Preissler, M., 1980. Ionic mechanisms of the glucose-induced membrane potential changes in β-cells. Horm. Metab. Res. (Suppl.) 10, 91–99.

Miura, R.M., Pernarowski, M., 1995. Correlations of rates of insulin release from islets and plateau functions for β-cells. Bull. Math. Biol. 57, 229–246.

Morris, C., Lecar, H., 1981. Voltage oscillations in the barnacle giant muscle fiber. Biophys. J. 35, 193–213.

Ozawa, S., Sand, O., 1986. Electrophysiology of endocrine cells. Physiol. Rev. 66, 887–952.

Pant, R.E., Kim, M., 1976. Mathematical descriptions of a bursting pacemaker neuron by a modification of the Hodgkin–Huxley equations. Biophys. J. 16, 227–244.

Satin, L.S., Cook, D.L., 1989. Calcium current inactivation in insulin-secreting cells is mediated by calcium influx and membrane depolarization. Pflügers Arch. 414, 1–10.

Sherman, A., Rinzel, J., 1991. Model for synchronization of pancreatic β-cells by gap junction coupling. Biophys. J. 59, 547–559.

Sherman, A., Rinzel, J., 1992. Rhythmogenic effects in weak electrotonic coupling in neuronal models. Proc. Natl. Acad. Sci. USA 89, 2471–2474.

Sherman, A., Rinzel, J., Keizer, J., 1988. Emergence of organized bursting in clusters of pancreatic β-cells by channel sharing. Biophys. J. 54, 411–425.

Sherman, A., 1994. Anti-phase, asymmetric and aperiodic oscillations in excitable cells-I. Coupled bursters. Bull. Math. Biol. 56, 811–835.

Smolen, P., Rinzel, J., Sherman, A., 1993. Why pancreatic islets burst but single β-cells do not. Biophys. J. 64, 1668–1680.

Terman, D., 1991. Chaotic spikes arising from a model of bursting in excitable membranes. SIAM J. Appl. Math. 51, 1418–1450.

Terman, D., 1992. The transition from bursting to continuous spiking in excitable membrane models. J. Nonlinear Sci. 2, 135–182.

Wang, X.-J., 1993. Genesis of bursting oscillations in the Hindmarsh–Rose model and homoclinicity to a chaotic saddle. Physica D 62, 263–274.

Yanchuk, S., Maistrenko, Y., Lading, B., Mosekilde, E., 2000. Chaotic synchronization in time-continuous systems. Int. J. Bifurcation and Chaos 10, 2629–2648.